Longitudinal- and transverse-wake-field effects in dielectric structures

M. Rosing and W. Gai
High Energy Physics Division, Argonne National Laboratory, Argonne, Illinois 60439
(Received 8 March 1990)

A dielectric-loaded circular waveguide structure is a potential high-gradient linear wake-field accelerator. A complete solution is given for the longitudinal electric and magnetic fields excited by a δ function and a Gaussian charge distribution moving parallel to the guide axis. The fields are then given in the limit of particle velocity equal to the speed of light. Example calculations are given for a structure with inner radius of 2 mm, outer radius of 5 mm, dielectric constant of 3, and total charge of 100 nC. Peak wake fields in excess of 200 MV/m are found. Azimuthal modes 0 and 1 are investigated for the particular interest of acceleration and deflection problems.

The electromagnetic radiation of a charged particle passing through a structure containing dielectrics[1,2] has many applications to accelerator physics. The next generation of electron-positron linear collides will require high-accelerating-gradient (> 100 MV/m) structures. Recently a new acceleration scheme, called the dielectric wake-field accelerator, has been proposed.[3] The concept of dielectric wake-field acceleration is very simple. It is a dielectric-lined waveguide and because of its slow wave characteristics it can be used as a wake-field device. In order to make the dielectric structure a practical wake-field acceleration device, however, one has to have high gradients and manageable transverse wake fields. The estimation of the transverse wake-field amplitudes in the dielectric structure is essential because it is directly related to the beam instability (or beam break-up mode) problem.[4] In this paper we calculate both the longitudinal and transverse wake fields produced in a dielectric structure by passing a charged particle. First we give a general expression for the wake fields corresponding to any particle velocity $\beta=v/c$ including all azimuthal modes m, then discuss the implication of the results under the limit of $\beta\rightarrow 1$, in particular for $m=0$ and 1.

We should point out that in our previous calculation[5] of the transverse wake field in the dielectric structure, we assumed that the vector potential $\mathbf{A}$ was proportional to the scalar potential ϕ. The implication of this assumption was that only TM-like wake fields would be excited, and that no TE-like wake field would exist. The consequence of this was that the higher-order azimuthal-mode $m\geq 1$ wake fields vanish when the electron beam is ultrarelativistic. This unexpected result attracted much interest in the community. Since then we continued calculations without preassumptions, as shown in this paper. In the meantime many other people[6-9] have also investigated this problem, and the results are that both TE and TM waves exist in the dielectric structure for $m\geq 1$ modes. The conclusion of all these works is that the transverse wake fields do not vanish even in the ultrarelativistic limit.

Consider the configuration of a metallic tube with inner radius b, partially filled with isotropic material with dielectric constant ϵ, containing a hole of radius a at the center which allows charged particles to pass through as shown schematically in Fig. 1. This structure is essentially an rf waveguide, having the usual rf waveguide characteristics. In our case we concentrate on the electromagnetic field radiated by a passing charged-particle beam. Consider a particle with charge e moving at velocity v along a line parallel to the axis of the tube at a distance r_0 as shown in Fig. 1. Because of the presence of the dielectric material, the Cherenkov radiation conditions will be satisfied when $\beta>\epsilon^{-1/2}$ and the particle will generate wake fields behind it. The wake fields produced by the motion of a charged particle are given by Maxwell's equations:

$$\nabla\times\mathbf{E}=-\frac{1}{c}\frac{\partial\mathbf{B}}{\partial t}\ ,\quad \nabla\cdot\mathbf{B}=0\ ,$$
$$\nabla\cdot\mathbf{D}=4\pi\rho,\quad \nabla\times\mathbf{H}=\frac{1}{c}\frac{\partial\mathbf{D}}{\partial t}+\frac{4\pi}{c}\mathbf{j}\ , \tag{1}$$
$$\mathbf{D}=\epsilon\mathbf{E},\quad \mathbf{B}=\mu\mathbf{H}\ .$$

From here on we will assume permeability $\mu=1$.

As a standard way of solving electrodynamic problems we introduce a scalar and a vector potential ϕ and $\mathbf{A}$, defined as

$$\mathbf{E}=-\nabla\phi-\frac{1}{c}\frac{\partial\mathbf{A}}{\partial t},\quad \mathbf{B}=\nabla\times\mathbf{A} \tag{2}$$

and choose the Lorentz condition

$$\nabla\cdot\mathbf{A}+\frac{1}{c}\frac{\partial\phi}{\partial t}=0\ . \tag{3}$$

The Maxwell equations can then be transformed into two uncoupled inhomogeneous wave equations, one for ϕ, one for $\mathbf{A}$:

$$\nabla^2\phi-\frac{\epsilon\mu}{c^2}\frac{\partial^2\phi}{\partial t^2}=-\frac{4\pi\rho}{\epsilon},\quad \nabla^2\mathbf{A}-\frac{\epsilon\mu}{c^2}\frac{\partial^2\mathbf{A}}{\partial t^2}=-4\pi\mathbf{j}\ . \tag{4}$$

For a charged particle moving at velocity v in the cylindrical coordinate z direction, the charge and current densities are

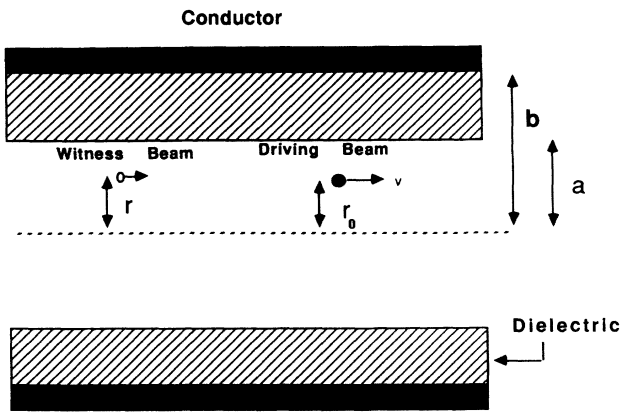

FIG. 1. A schematic dielectric weak-field structure.

$$\rho=\frac{e\delta(r-r_0)}{r}\delta(\theta)\delta(z-vt),\quad \mathbf{j}=\mathbf{v}\rho\ . \tag{5}$$

First we solve for the potential in the vacuum hole. In this case $\epsilon=1$ and $\mu=1$. Expanding the δ functions

$$\frac{\delta(r-r_0)}{r}\delta(\theta)=\frac{1}{2\pi}\sum_{m=-\infty}^{\infty}e^{im\theta}\int_0^\infty J_m(kr)\times J_m(kr_0)k\,dk\ , \tag{6}$$

$$\delta(z-vt)=\frac{1}{2\pi v}\int_{-\infty}^{\infty}e^{i(\omega/v)(z-vt)}d\omega\ , \tag{7}$$

the charge density $\rho(r,\theta,z,t)$ can be written as

$$\rho(r,\theta,z,t)=\frac{e}{(2\pi)^2 v}\sum_m\int\int\rho_m(r,\theta,z,t,k,\omega)\times k\,dk\,d\omega\ , \tag{8}$$

it is easy to show that ρ_m satisfies the wave equation (4):

$$\nabla^2\rho_m-\frac{1}{c^2}\frac{\partial^2\rho_m}{\partial t^2}=\lambda\rho_m\ ; \tag{9}$$

i.e., it is an eigenfunction of the d'Alembertain operator with eigenvalue $\lambda=-[k^2+(\omega/c)^2(1-\beta^2)]$. It is straightforward to show that the inhomogeneous solution of the wave equation is

$$\begin{aligned}\phi(\mathbf{r},z,t)&=\frac{e}{\pi v}\sum_{m=-\infty}^{\infty}e^{im\theta}\int_0^\infty\int_{-\infty}^{\infty}\frac{J_m(kr)J_m(kr_0)e^{i(\omega/v)(z-vt)}}{[k^2+(\omega/c)^2(1-\beta^2)]}d\omega\,k\,dk\\&=\frac{1}{v}\sum_m e^{im\theta}\int e^{i(\omega/v)(z-vt)}\phi_{m,\text{inhom}}(r,\omega)d\omega\ ,\end{aligned} \tag{10}$$

where

$$\phi_{m,\text{inhom}}(r,\omega)=\frac{e}{\pi}K_m\left[\frac{\omega}{v}\sqrt{1-\beta^2}r_>\right]\times I_m\left[\frac{\omega}{v}\sqrt{1-\beta^2}r_<\right]\ . \tag{11}$$

By the same method we can show that the inhomogeneous solution for A_z is

$$A^m_{z,\text{inhom}}=\frac{v}{c}\phi_{m,\text{inhom}}\ . \tag{12}$$

To simplify the notation, we introduce the symbols

$$k^2=\frac{\omega^2}{v^2}(1-\beta^2)\ , \tag{13}$$

$$s^2=\frac{\omega^2}{v^2}(\epsilon\beta^2-1)\ , \tag{14}$$

$$k_0=\frac{\omega}{c}\ . \tag{15}$$

The above inhomogeneous solutions are combined with the homogeneous solution of the wave equation to form a complete solution. Any potential and field component $f(r,\theta,z,t)$ can be expressed in terms of its Fourier transform $f^m(r,\omega)$, i.e.,

$$f(r,\theta,z,t)=\int_{-\infty}^{\infty}\sum_m e^{im\theta}f^m(r,\omega)e^{i(\omega/v)(z-vt)}d\omega\ . \tag{16}$$

Again for simplicity we shall write all the Fourier-transformed potential and field components $f^m(r,\omega)$ as f^m unless otherwise noted. We find the complete solutions to Eq. (4) to be, for $r<a$,

$$\varphi_m=\frac{e}{\pi}[I_m(kr_<)K_m(kr_>)+a'_mI_m(kr)]\ , \tag{17}$$

$$A^m_z=\frac{e}{\pi}\beta[I_m(kr_<)K_m(kr_>)+c'_mI_m(kr)]\ , \tag{18}$$

$$A^m_\theta=i\frac{e}{\pi}\beta\left[g'_m\frac{m}{kr}I_m(kr)-e'_mI'_m(kr)\right]\ , \tag{19}$$

$$A^m_r=\frac{e}{\pi}\beta\left[g'_mI'_m(kr)-e'_m\frac{m}{kr}I_m(kr)\right]\ , \tag{20}$$

and, for $r>a$,

$$\phi_m=\frac{e}{\pi\epsilon}[a_mJ_m(sr)+b_mN_m(sr)]\ , \tag{21}$$

$$A^m_z=\frac{e}{\pi\epsilon}\beta[c_mJ_m(sr)+d_mN_m(sr)]\ , \tag{22}$$

$$A^m_\theta=i\frac{e}{\pi\epsilon}\beta\left[g_m\frac{m}{sr}J_m(sr)+e_mJ'_m(sr)+h_m\frac{m}{sr}N_m(sr)+f_mN'_m(sr)\right]\ , \tag{23}$$

$$A_r^m=\frac{e}{\pi\epsilon}\beta\left[g_m J_m'(sr)+e_m\frac{m}{sr}J_m(sr)+h_m N_m'(sr)+f_m\frac{m}{sr}N_m(sr)\right], \tag{24}$$

where a_m',c_m',e_m',g_m' and $a_m,b_m,c_m,d_m,e_m,f_m,g_m,h_m$ are the constants yet to be determined by the boundary conditions.

All the electromagnetic-field components can be expressed in terms of ϕ and $\mathbf{A}$: i.e.,

$$E_z^m=i\frac{k_0}{\beta}(\phi_m-\beta A_z^m), \tag{25}$$

$$E_\theta^m=-i\frac{m}{r}\phi_m-ik_0A_\theta^m, \tag{26}$$

$$E_r^m=-\frac{\partial\phi_m}{\partial r}-ik_0A_r^m, \tag{27}$$

$$H_z^m=\frac{\partial A_\theta^m}{\partial r}+\frac{A_\theta^m}{r}-i\frac{m}{r}A_r^m, \tag{28}$$

$$H_\theta^m=-i\frac{k_0}{\beta}A_r^m-\frac{\partial A_z^m}{\partial r}, \tag{29}$$

$$H_r^m=i\frac{m}{r}A_z^m+i\frac{k_0}{\beta}A_\theta^m. \tag{30}$$

Using boundary conditions $E_z=E_\theta=0$ at $r=b$, E_z,E_θ,D_r,H_z continuous at $r=a$, and the Lorentz condition, one can solve for all the unknown coefficients. The mathematics of solving for the coefficients is straightforward but very long. We will omit the details here and only give the results. The details can be found in Ref. 10. For the longitudinal electric and magnetic fields of any given mode m, the results are

$$E_z^m(r,\theta,z_0)=-8e\cos(m\theta)\cos\left[\frac{k_0}{\beta}z_0\right]\times I_m(kr)I_m(kr_0)\times\frac{K_m(ka)}{I_m(ka)}\frac{T(s)}{s\,dC(s)/ds}\bigg|_{s=s_\lambda}, \tag{31}$$

$$H_z^m(r,\theta,z_0)=-8e\sin(m\theta)\sin\left[\frac{k_0}{\beta}z_0\right]\times I_m(kr)I_m(kr_0)\frac{K_m(ka)}{I_m(ka)}\times\frac{T(s)}{s\,dC(s)/ds}\bigg|_{s=s_\lambda}, \tag{32}$$

where

$$T(s)=s^2k^2\left[\frac{kS_m'(sa)}{S_m(sa)}+\frac{sI_m'(ka)}{I_m(ka)}\right]\times\left[\frac{sK_m'(ka)}{K_m(ka)}+\frac{\epsilon kR_m'(sa)}{R_m(sa)}\right]-\frac{m^2}{a^2}k^4\beta^2\left[\frac{\epsilon-1}{1-\beta^2}\right]^2, \tag{33}$$

$$C(s)=\frac{m^2sk^2}{a^2}\beta^2\left[\frac{\epsilon-1}{1-\beta^2}\right]^2-s^3\left[\frac{kS_m'(sa)}{S_m(sa)}+\frac{sI_m'(ka)}{I_m(ka)}\right]\times\left[\frac{sI_m'(ka)}{I_m(ka)}+\frac{\epsilon kR_m'(sa)}{R_m(sa)}\right], \tag{34}$$

and

$$R_m(sr)=N_m(sb)J_m(sr)-J_m(sb)N_m(sr), \tag{35}$$

$$R_m'(sr)=N_m(sb)J_m'(sr)-J_m(sb)N_m'(sr), \tag{36}$$

$$S_m(sr)=N_m'(sb)J_m(sr)-J_m'(sb)N_m(sr), \tag{37}$$

$$S_m'(sr)=N_m'(sb)J_m'(sr)-J_m'(sb)N_m'(sr), \tag{38}$$

where $f'(x)=df(x)/dx$ and J_m and N_m are mth-order Bessel functions of the first and second kinds, respectively, and $z_0=z-vt$ is the distance behind the charge. s_λ are the zeros of $C(s)$.

The function $C(s)$ is termed the conditional equation. The radiated electromagnetic field (with phase velocity v) will satisfy $C(s_\lambda)=0$, which agrees with Chang and Dawson's results.[11] All the other field components can be derived from E_z and H_z.

So far we have solved the complete electromagnetic fields radiated by a single charged particle, even though the form of the solutions is very complicated. Next we will discuss some special cases, especially for $m=0,1$ and under the limit of $\beta\to1$ or $\gamma\to\infty$.

For $m=0$ and $\beta\to1$, Eq. (31) can be simplified as

$$E_z(r,z_0)=\frac{4e}{\epsilon a}\sum_\lambda\left[\frac{R_0(sa)}{\frac{d}{ds}\left[R_0'(sa)-\frac{sa}{2\epsilon}R_0(sa)\right]}\right]_{s=s_\lambda}\times\cos\left[\frac{\omega_\lambda}{c}z_0\right], \tag{39}$$

$$H_z(r,z_0)=0, \tag{40}$$

where s_λ satisfies the condition

$$R_0'(sa)-\frac{sa}{2\epsilon}R_0(sa)=0 \tag{41}$$

and z_0 is the distance behind the charge.

The transverse wake fields can be directly calculated from E_z by using the Panofsky-Wenzel theorem[12]

$$\frac{\partial \mathbf{F}_\perp}{\partial z} = e\nabla_\perp E_z \ , \tag{42}$$

which gives

$$F_r = e(E_r - \beta B_\theta) = e\int \frac{\partial E_z}{\partial r} dz \ , \tag{43}$$

$$F_\theta = e(E_\theta + \beta B_r) = e\int \frac{\partial E_z}{r\partial \theta} dz \ . \tag{44}$$

For a Gaussian line charge with rms bunch length σ, the wake fields can be expressed as the integration

$$E_z^m(r,\theta,z_0) = \frac{N}{\sigma\sqrt{2\pi}} \int_{-\infty}^{z_0} E_z^m(r,\theta,z) e^{-[(z_0-z)/\sigma]^2} dz \ , \tag{45}$$

where N is the total number of charges in the driving bunch and z_0 is the distance behind the center of the driving bunch where the field is measured. A discussion of a few examples is given below.

The axial electric field given by (39) and (45) is of interest for the dielectric wake-field accelerator because it can indicate a very high acceleration gradient which is one of the requirements for the next generation of linear colliders. As an example, an electron bunch with 100 nC total charge and rms bunch length σ of 1 mm passing through a structure with $a=0.2$ cm, $b=0.5$ cm, and dielectric constant $\epsilon=3$ produces a peak accelerating gradient $E_z=240$ MeV/m. The complete wake is plotted in Fig. 2 where the dotted line is the longitudinal distribution of the driver beam. One should notice that there is no r dependence of E_z in (39) and by applying the Panofsky-Wenzel theorem, there will be no transverse focusing force. The transverse beam profile will not be influenced by the wake fields in the $m=0$ mode.

For $m \geq 1$ modes and $\beta \to 1$, the longitudinal electric and magnetic fields [Eqs. (31) and (32)] become

$$E_z^m(r,\theta,z_0) = -\frac{4e}{a^2 D(s_\lambda)} \left[\frac{r_0 r}{a^2}\right]^m \cos(m\theta)\cos(k_0 z_0) \ , \tag{46}$$

$$H_z^m(r,\theta,z_0) = -\frac{4e}{a^2 D(s_\lambda)} \left[\frac{r_0 r}{a^2}\right]^m \sin(m\theta)\sin(k_0 z_0) \ , \tag{47}$$

where

$$D(s) = \frac{-s}{2ma^2}\frac{dC}{ds} \ . \tag{48}$$

The conditional equation (34) can be rewritten in the $\beta \to 1$ limit as

$$C(s) = \frac{m(\epsilon+1)}{s^2 a^2} - \frac{1}{m+1} - \frac{1}{sa}\left[\frac{S_m'(sa)}{S_m(sa)} + \epsilon\frac{R_m'(sa)}{R_m(sa)}\right] \ . \tag{49}$$

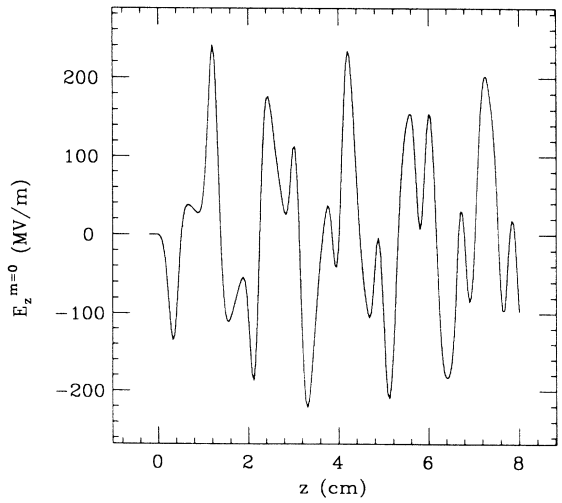

FIG. 2. Longitudinal-wake-field effect for $m=0$. The first four modes were used in the summation, all the higher modes do not contribute significantly.

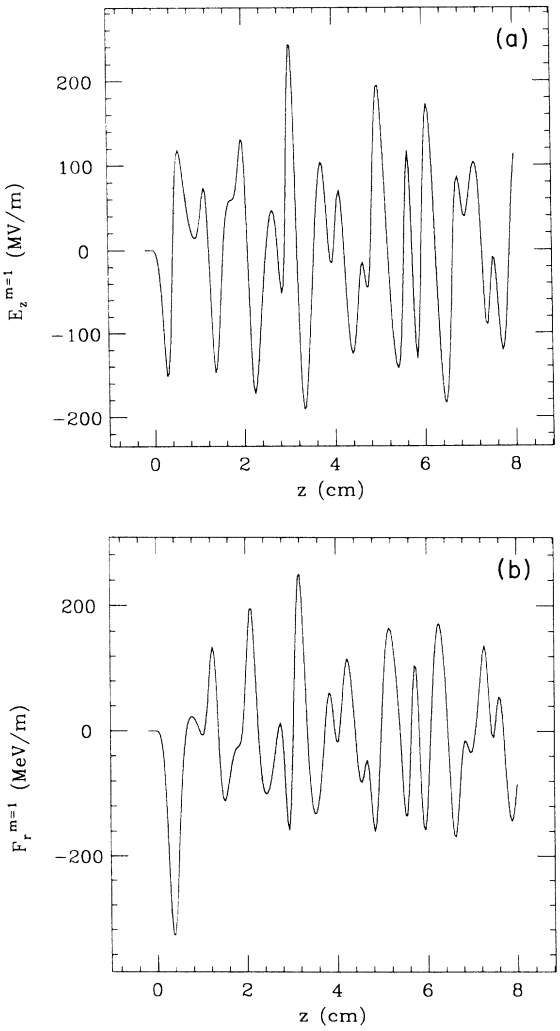

FIG. 3. (a) Longitudinal wake field for $m=1$ at $r=r_0=a$; the first four modes were used. (b) Transverse wake field F_f for $m=1$ at $r=r_0=a$; the first four modes were used.

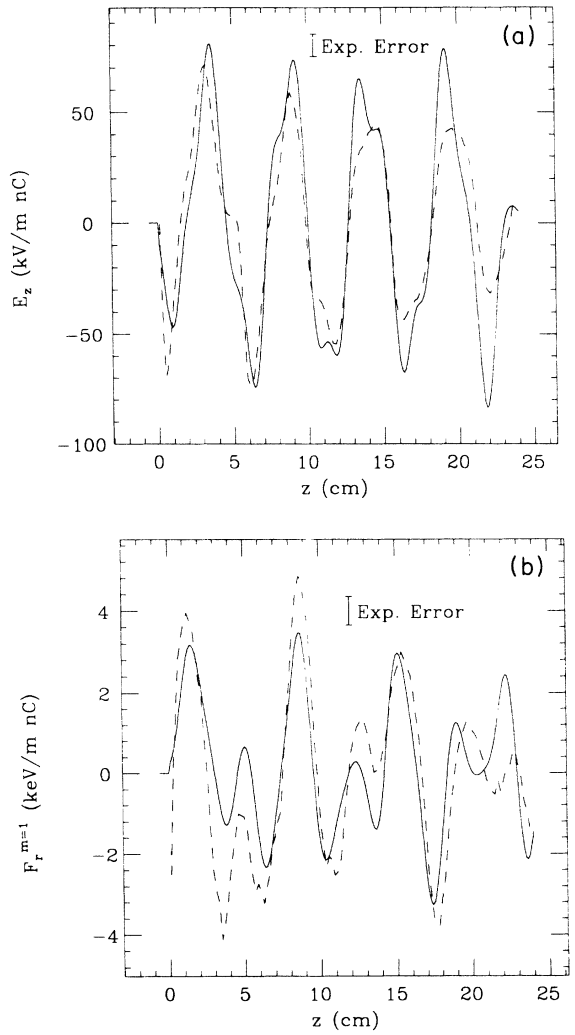

FIG. 4. Comparison of experimental data with calculations for longitudinal and transverse wakes. The dashed line represents data and the solid line theory (first four modes). (a) Longitudinal E_z. (b) Transverse F_r.

The numerical example of the $m=1$ longitudinal and transverse wake field for the parameters of Fig. 2 is shown in Fig. 3. The beam profile is the line distribution. The wake fields were evaluated at $r=r_0=a$. As seen in Fig. 3(b), an off-centered electron beam will leave a transverse deflection force behind it. The amplitude of the longitudinal wake for $m=1$ is comparable to the $m=0$, longitudinal wake field shown in Fig. 2. As seen in Eq. (46) the magnitude of the transverse field is proportional to the off-center distance r_0. This will imply some restrictions on the direct application of the dielectric wake field as a high-energy accelerator, particularly on beam alignment. It will be essential and critical to align the drive beam close to the axis, so that the beam break up[4] (BBU) will be controlled and also the accelerated beam will not be deflected away.

We have compared our calculated results with the recent experiment[13] performed at the Advanced Accelerator Test Facility (AATF) at Argonne National Laboratory,[14] where the wake fields of a drive beam are sampled by a separate witness beam. For the experimental setup we have used $b=2.22$ cm, $a=1.27$ cm, and the dielectric material was Lucite which has dielectric constant of 2.6. The rms electron bunch length of the driving and witness beams are 3 mm. Both experimental results and calculations are normalized to 1 nC charge and 1-m-long structure. In the experiment, the driving beam was purposely steered off center for $r_0=1$ mm. Figure 4(a) shows the comparison of the longitudinal wake field between the experiment and calculation from Eq. (31). Figure 4(b) is the transverse wake field for $m=1$ from Eqs. (31) and (43). As seen, our calculated results are in very good agreement with the experiment, both qualitatively and quantitatively. We have also compared the dielectric structure with an iris-loaded metallic structure. For the given a,b and same offset r_0, the magnitude of transverse wake field relative to longitudinal wake field is smaller in the dielectric than in the iris-loaded metallic structure.[13]

In summary, we have calculated the wake-field effects in a dielectric structure and a general formula is given for all composite modes at any charged-particle velocity β. We have investigated the particular cases of $m=0$ and $m=1$. The important conclusion is that the longitudinal and transverse wake fields excited by a charged-particle beam passing through a dielectric-lined tube do not vanish, even under the limit of $\beta\rightarrow 1$. An example, given for a particular high-frequency structure, indicates that careful alignment is required to minimize the transverse wake-field effects. Direct application of a dielectric wake field device as a practical accelerator is possible even though the transverse fields present a problem. Further study is needed to deal with all the accelerator issues, both theoretically and experimentally.

We would like to thank P. Schoessow, J. Norem, E. Chojnacki, S. Mtingwa, J. Rosenzweig, M. Jones, K. Ng, and R. Gluckstern for useful discussions. Also we would like to thank J. Simpson for his helpful discussion and encouragement throughout these investigations. This work was supported by the Department of Energy, High Energy Physics Division, Contract No. W-31-109-ENG-38.

[1]B. M. Bolotovskii, Usp. Fiz. Nauk **75**, 295 (1961) [Sov. Phys. Usp. **4**, 781 (1962)].

[2]A. Piwinski, DESY Report No. 72/72, 1972 (unpublished).

[3]R. Keinigs, M. E. Jones, and W. Gai, Part. Accel. **24**, 223 (1989).

[4]P. Wilson, in *Physics of High Energy Particle Accelerators,* Lectures from the Summer School on High Energy Particle Accelerators, edited by R. A. Carrigan, F. R. Huson, and M. Month (AIP Conf. Proc. No. 87) (AIP, New York, 1982), p. 450.

[5]W. Gai, in *Advanced Accelerator Concepts,* proceedings of the Workshop, Lake Arrowhead, California, 1989, edited by

Chan Joshi (AIP Conf. Proc. No. 193) (AIP, New York, 1989), p. 111.
[6]M. Jones, R. Keinigs, and W. Peter, Los Alamos Report No. LUR-89-4234 (unpublished).
[7]K. Y. Ng, this issue, Phys. Rev. D **42**, 1819 (1990).
[8]R. Gluckstern (private communication).
[9]E. Garate (private communication).
[10]M. Rosing, Argonne National Laboratory report No. WF-131, 1989 (unpublished).
[11]C. Chang and J. Dawson, J. Appl. Phys. **41**, 4493 (1970).
[12]W. K. H. Panofsky and W. A. Wenzel, Rev. Sci. Instrum. **27**, 967 (1956).
[13]E. Chojnacki, W. Gai, C. Ho, R. Konecny, S. Mtingwa, J. Norem, M. Rosing, P. Schoessow, and J. Simpson (unpublished).
[14]H. Figueroa, W. Gai, R. Konecny, J. Norem, A. Ruggiero, P. Schoessow, and J. Simpson, Phys. Rev. Lett. **60**, 2144 (1988).